Two-phase modelling and simulation of the hydrothermal fractionation of holm oak in a packed bed reactor with hot pressurized water

*A. Cabeza, F. Sobrón, F.M. Yedro, and J. García-Serna**

High Pressure Processes Group, Department of Chemical Engineering and Environmental Tech., University of Valladolid, 47011 Valladolid, Spain

**Corresponding author: Tel.: +34 983184934*
E-mail: jgserna@iq.uva.es (J. García-Serna)

Abstract

Hydrothermal fractionation has been thoroughly studied in order to develop a sustainable process to recover the sugars or the biopolymers contained in biomass. However, a physico-chemical model which considers the main involved physical phenomena, like porosity variations, has not been fully developed. Thus, the objective of this work was to approach a more realistic model than other yet published, incorporating also a novel reaction pathway for biomass fractionation. It establishes that cellulose and hemicellulose begin their fractionation in the solid, breaking in water-soluble oligomers and sugar. Besides, deacetylation reactions and insoluble oligomer formation from cellulose were considered. Kinetics followed the Arrhenius' law and and it has been demonstrated that an autocatalytic kinetic model can be successfully used to simulate the biomass breaking in soluble oligomers. The process was carried out in a tubular reactor charged with 5 g of holm oak and continuously fed with hot pressurized water. To assess the mass transfer between the solid and liquid, 4 volumetric flows (5mL/min, 10mL/min, 20mL/min and 40 mL/min) and two particle diameters (3mm and 6mm) were used. In the same way, temperature was set between 175ºC and 207ºC. The latter was the main variable due to its effect in biomass solubility and kinetics. The model was solved by the Runge-Kutta's method with 8^{th} order of convergence and its discretization was performed by a new modification of the orthogonal collocation method on finite elements. It was validated by fitting total organic carbon (TOC) with Absolute Average Deviation (A.A.D. between 16.3% and 55.8%), acetic acid concentration (A.A.D. between 44.4% and 84.4%) and pH profiles (A.A.D. between 5.6% and 9.7%). Besides, the mass transfer between the solid and the liquid was checked and the deviations of the simulation were lower than 8.5%.

Keywords: Autocatalytic kinetic, two-phase simulation, holm oak, hydrothermal fractionation, packed bed reactor.

1. Introduction

For several decades petrol has been used as the main source of energy and raw material. Nevertheless, it is not a sustainable source and other option will be needed in a near future. One likely option would be biomass, and several international institutions, such as the European Union or the Organisation for Economic Co-operation and Development, have shown interest about it (King, 2009; OCDE, 2009; Organisation, 2011). The general idea is to develop a hydrolysis process to obtain the sugars present in biomass, which will be converted into liquid fuels in a following process. In addition, the extraction of the biomass phenolic compounds would be interesting due to the fact that they would be used as raw material to chemical industry. Thus, biomass hydrolysis have been studied thoroughly and in different ways, such as, enzymatic hydrolysis, acid or alkaline hydrolysis (Alvarez-Vasco and Zhang, 2013; Charles et al., 2004; Feng et al., 2012; Gao et al., 2013; Yoon et al., 2014). One of the most promising option would be the biomass fractionation by hydrothermal processes, as at subcritical conditions as at supercritical conditions, because they can extract the main fraction of these sugars only using water as reactive (Cantero et al., 2013; Garrote et al., 2002; M. Sefik Tunc, 2008; Moniz et al., 2013; Parajó et al., 2004; Rissanen et al., 2014; Zakaria et al., 2015). Subcritical conditions refer to all temperature and pressure below the critical point and, supercritical conditions, when they are beyond it (Figure 1). Focusing in water, subcritical water means a liquid at high pressure and temperature what provide it special properties, such as lower dielectric constant and densities (Asl and Khajenoori, 2013; Franck, 1970; Kruse and Dinjus, 2007; Teo et al., 2010).

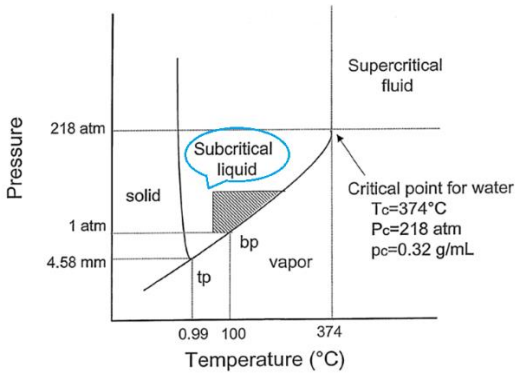

Figure 1: Phase diagram of water P-T (Asl and Khajenoori, 2013). tp: triple point, bp: boiling point, T_c, P_c and ρ_c: critical temperature, pressure and density respectively.

Regarding modelling, some studies have been performed in order to establish a reaction pathway and kinetic equations to reproduce the experimental behaviour of the hydrolysis reactors. All of them consider that biomass is formed by three polymeric fractions: cellulose, hemicellulose and lignin. Cellulose and hemicellulose are sugar-based biopolymers and lignin is an aromatic biopolymer formed by phenylpropane units. Cellulose and hemicellulose are differentiated by their structure and composition. The former is a linear polymer constituted by hexoses and the latter is an amorphous and branched polymer of hexoses and pentoses (Bobleter, 1994; P. Harmsen, 2010). The most extended models are based on first order kinetics to cellulose and hemicellulose assuming that they decompose into intermediate oligomer products. These oligomers would continue a further bond cleavage generating the final monomeric sugars (pentose and hexoses). In addition, the degradation of these sugars into several acids can be considered (Charles et al., 2004).

Sandra Rivas et al. (Rivas et al., 2014) studied the acidic processing of hemicellulosic saccharides from pine wood and they developed a monophasic globalised kinetic model with first order kinetics respect to the biomass. That model was suitable to fit their experimental data, R^2 between 0.975 and 0.998. *Sasaki et al.* (Sasaki et al., 2002) assessed the kinetic and mechanism of cellobiose (disaccharide composed by two glucoses) hydrolysis. This monophasic model again used first order kinetics and it could reproduce the experimental behaviour. *Pronyk and Mazza* (Pronyk and Mazza, 2010) developed a kinetic model with first order kinetics to the hemicellulose hydrolysis from Triticale Strawa in a packed bed reactor, taking into account the mass transfer between solid and liquid. They assumed that two types of hemicellulose can be present, one easily degradable and other hardly degradable. They considered that the porosity of the bed remains constant during the process too. *Jussi V. Rissanen et al.* (Rissanen et al., 2014) studied the extraction of spruce hemicellulose and they developed a kinetic model which could reproduce the experimental behaviour in a cascade fluidised batch reactor, using kinetics of n^{th} order to solid biomass. Moreover, they also considered the proton concentration in kinetics (with n^{th} reaction order too) because acetic acid and other organics are produced and solved during the extraction. Therefore, there are several models which deal with biomass hydrothermal fractionation and they have obtained good results. However, they are focused in hemicellulose or cellulose fractionation and not in both of them at the same time. In addition, they do not consider some observed physical phenomena, such as, porosity changes in a bed reactor or protons effect in all kinetics in liquid phase.

Thus, the aim of this article was to develop a new kinetic model for biomass hydrothermal fractionation which could reproduce the global experimental behaviour in the most realistic way as it was possible. Trying to understand how this hydrothermal reaction takes place and analysing the effect of the particle diameter, operating temperature and liquid flow rate. So, it was taken into account the effect of pH, porosity variations and solubility of the different biomass fractions in hot water (Kruse and Dinjus, 2007; Miller-Chou and Koenig, 2003; Teo et al., 2010) in a novel reaction pathway. The selected reactor was a tubular reactor, in order to study the process in a semi-continuous process, fed with hot pressurized water. The studied biomass was holm oak because it is one of the most common trees in the south of Spain and wastes, which could be used as raw material, are produced each year during its pruning. Regarding kinetics, a new formulation was incorporated too. An autocatalytic model is considered because it was assessed, in a previous study about biomass thermal degradation during a thermogravimetric analysis (Cabeza et al., 2015), that it can reproduce the strong mass changes in biomass at certain times or temperatures.

2. Experimental

2.1. Material and methods

2.1.1. Raw materials

Holm Oak branches were selected as studied biomass because it is one of the main source of woody wastes in the southern Spain. It was characterized by the National Renewable Energy Laboratory (NREL) – Determination of Structural Carbohydrates and Lignin in Biomass- standards. In order to check the reproducibility, the method was applied three times. The biomass was dried and milled in the selected diameters, 3 and 6 mm. Extractives were calculated gravimetrically by Soxhlet method according to the Determination of Extractives in Biomass. The initial composition of the biomass

sample is collected in Table 1. The value of the lignin includes the extractive lignin (2.36%) and the acid soluble lignin (1.05%).

Table 1: Initial composition of the holm oak sample

Cellulose g/g	Hemicellulose g/g	Lignin g/g
0.4806	0.2060	0.3134

All chemicals were provided by Sigma. The reactive compounds for the HPLC analysis were: cellobiose (+98%), glucose (+99%), fructose (+99%), glyceraldehyde (95%), pyruvaldehyde (40%), arabinose (+99%), 5-hydroxymethylfurfural (99%), lactic acid (85%), formic acid (98%), acrylic acid (99%), mannose (+99%), xylose (+99%), levulinic acid (+99%) and galactose (+99%). For analysis of carbohydrates and lignin, sulfuric acid (98%) and calcium carbonate (≥ 99.0%) were used. For the determination of extractives n-hexane (95%) was selected as solvent. Distilled water was used in all assays.

2.1.2. Experimental device

The hydrothermal fractionation process was carried out in a semibatch reactor charged with approx. 5 g of dry holm oak. To avoid particle losses two metallic filters were used, which were located at the top and bottom of the reactor. The reactor (R-01) was a microtube model SS316 piping with a length of 38 cm and an external diameter of ½ inch. This reactor and a preheater (E-02, AISI 316, length=200 cm, O.D.=1/8 inch) were introduced inside a chromatographic oven HP568 (F-01). The system was fed by a Jasco model PU-2080 pump (P-01) and the pressure was set using a go-backpressure valve (V-01) to maintain the liquid phase. Aimed at saving energy, a concentric tube heat exchanger (E-01, 1/4”-3/8”) of 70 cm was installed before the input oven (heat integration). Finally, a second concentric tube heat exchanger (E-03, 1/4”-3/8”) of 15 cm was used to cool the product flow down to room temperature (25-30ºC). A process flow diagram of the pilot plant is shown in Figure 2.

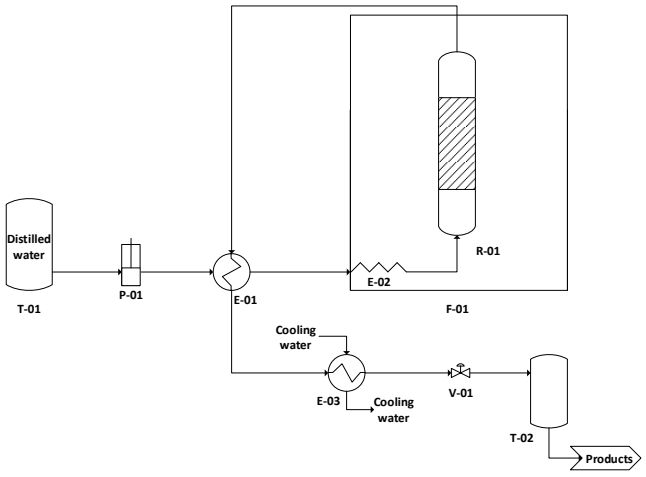

Figure 2: Process flow diagram of the pilot plant. T-01: feed water tank, P-01: feed pump, E-01: heat recover, F-01: oven. E-02: feed preheater, R-01: packed bed reactor. E-03: cooler, V-01: backpressure valve and T-02: sample tank.

Samples of the output liquid were taken from the tank T-02 measuring pH, total organic content (TOC) and acetic acid concentration. The solid inside of the reactor was collected and quantified too. The analytical methods are described next.

2.1.3. Solid phase characterization. Lignin and sugar content

The solid phase characterization was done following the method provided by the National Renewable Energy Laboratory (NREL) – Determination of Structural Carbohydrates and Lignin in Biomass. Therefore, a sample of 300 mg (m_i) was treated with 3 mL of sulphuric acid (72%) followed by an incubation of 30 min at 30ºC. Then, 84 mL of distilled water were introduced and it was incubated for one hour at 121ºC. The resultant suspension was filtered under vacuum, washing with distilled water, and dried at 105ºC for 24 h. Then, the solid was weighted (m_1) and calcined at 550ºC for 24 h and weighted (m_2) again. So, the acid insoluble lignin would obtained by $(m_1 - m_2)/m_i$. The recovered liquid was used to obtain the content of acid soluble lignin by spectrophotometry, measuring the absorbance at 320 nm and using the recommended absorptivity at a wavelength of 30 $l \cdot g^{-1} \cdot cm^{-1}$. In addition, 30 mL were neutralized with calcium carbonate up to pH=6-7 followed by a filtering using 0.2 µm filters and finally analysed by high pressure liquid chromatography (HPLC). The used HPLC column was SUGAR SH-1011 (Shodex). The mobile phase was a solution of 0.01N of sulfuric acid and Milli-Q water. In order to obtain the hemicelluloses, celluloses and degradation product from sugars content two detector were used: a Waters IR detector 2414 (210 nm) and Waters dual λ absorbance detector 2487 (254 nm).

2.1.4. Liquid phase characterization

The hydrothermal fractionation of biomass generates a complex mixture of sugars and oligomers, which is difficult to analyse. So, an acid hydrolysis was performed to convert these oligomers into their monomeric sugars. Samples of 10 mL were hydrolyzed adding 4 mL of sulphuric acid and they were incubated for 30 min at 30ºC. After, 86 mL of distilled water were added and the sample was incubated for one hour more at 121ºC. Then, it was neutralized with calcium carbonate until pH=6-7 and filtered using 0.2 µm filters. Finally, it was analysed by HPLC as explained in the before section.

In addition, the pH and total organic carbon (TOC) were measured. The pH was determined by Nahita model 903 and the TOC was measured by Shimadzu equipment model TOC-VCSH. The carbon concentration of the standard solutions corresponds to 500 mg C/L.

2.2. Procedure

2.2.1. Effect of the volumetric flow

The effect of the liquid flow was assessed by performing 4 experiments at different volumetric flows (5 mL/min, 10 mL/min, 20 mL/min and 40 mL/min) for two intervals of temperature, one around 180 ºC and another around 190 ºC. Pressure was maintained at 100 barg to ensure the liquid phase of the water. The aim was to analyse how the mass transfer is modified with the inflow.

2.2.2. Effect of the particle diameter

In order to study how the particle diameter affects to the process two diameters were used, 3 mm and 6 mm. This parameter has importance because it affects directly the mass transfer and the overall process due to the changes in the solid porosity.

2.2.3. Effect of the operating temperature

Experiments from 175ºC and 207ºC were performed divided in three sets. One set of three cases around 180ºC, other three around 190ºC and two at 207ºC. The idea was to analyse how small changes in temperature affect the biomass degradation in terms of solubility, as kinetics has been considered in other studies (Cantero et al., 2013; Rissanen et al., 2014; Sasaki et al., 2002).

All the experiments and their operational conditions are shown in Table 2.

Table 2: Operational conditions of the performed experiments

Experiment	Operating Temperature ºC	Particle diameter mm	Real flow mL/min	Initial mass g	Operating time min
1	175	3	3.8	5.3124	94
2	207	3	9.6	5.3207	94
3	185	3	17.8	5.3308	94
4	180	3	32.7	5.2603	94
5	190	6	2.4	5.2637	94
6	207	6	9.5	5.4993	94
7	195	6	19.3	5.2520	94
8	180	6	34.9	5.2207	94

2.2.4. Model validation

The aim of the model is to reproduce the general behaviour of the system, considering temperature, flow, particle diameter, pH and the main biopolymers and oligomers during the reaction. For this reason, the TOC and the pH of each experiment were measured and fitted. In addition, acetic acid concentration in liquid phase was considered in the experiments with a particle diameter of 3 mm. The latter was taking into account because this compound would be the main source of protons and, for this reason, the basis of the autohydrolysis. Sugar concentration in liquid phase was only simulated in order to check if the simulation agrees with the behaviour reported by other authors.

3. Modelling

3.1. Hydrothermal degradation at subcritical conditions

Biomass fractionation starts in solid phase with hemicellulose and cellulose cleavage into oligomers of decreasing molecular weight. In both cases, at a certain polymer length they became water-soluble, being solubilised. These solubilised oligomers suffer a further hydrolysis process and they continue degrading in smaller oligomers down to their respective monomers. Finally, these monomers (mainly reduced sugars) can break into several degradation products, such as hydroxymethylfurfural, furfural, formic acid, lactic acid and others (Alvarez-Vasco and Zhang, 2013; Feng et al., 2012). An

illustration of this hydrothermal degradation with the evolution of the solid and liquid phase with time and along the reactor is schematised in Figure 3. Once the reactor was fed, water would start to degrade and to solve biomass. Thus, it is expected that, because of this extraction, the size of the particle starts to decrease, starting in the feed of the reactor. The reactor behaved like a fixed bed extraction column, thus, solid is depleted from bottom to top and liquid is more concentrated at the outlet (top exit in this case).

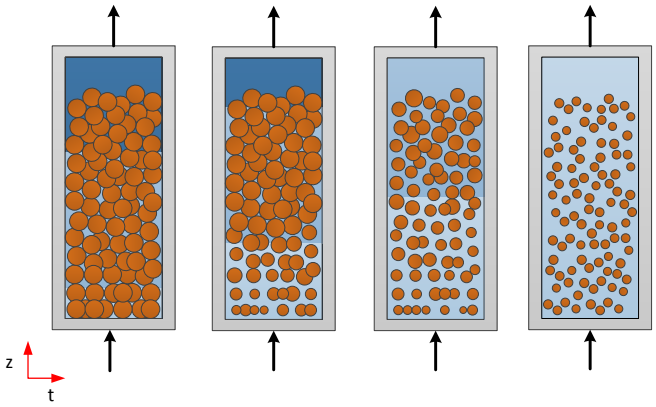

Figure 3: Expected behaviour in liquid and solid phase inside the hydrothermal reactor.

3.2. Biomass solubility

The solubility of polymers in water mainly depends on three factors: molecular weight, crystallinity and amount of active groups. The higher the crystallinity and the molecular weight are, the lower the solubility is. However, concentration of active groups enhances water solubility (Miller-Chou and Koenig, 2003). Cellulose is insoluble in water due to its crystallinity and its low acetylation degree, so only oligomers with a very low molecular weight would be water soluble. Nevertheless, at high temperatures water dielectric properties have a tremendous change which could enhance cellulose solubility (Franck, 1970; Kruse and Dinjus, 2007; Teo et al., 2010). For example, its relative value changes, at 25 MPa, from 83 at 25 ºC to 43 at 207 ºC, and from 81 to 33 at the same temperatures and 100 bar. In contrast, hemicellulose has a lot of acetyl groups in its structure and it is amorphous. So, it is expected that hemicellulose oligomers with high molecular weight could be solubilised. On the other hand, lignin is a complex structure and some parts could be soluble.

3.3. Autohydrolysis

Another process that takes place in the reactor is the deacetylation of hemicellulose (Garrote et al., 2002; Parajó et al., 2004) and cellulose (Gao et al., 2013), which release acetic acid from de solid to the liquid phase. This emission of acetic acid implies a higher amount of protons in the liquid phase, enhancing the hydrolysis reactions in this phase.

3.4. Reaction pathway

The reaction mechanism is shown in Figure 3.The idea was to develop a pathway which would be able to represent the main phenomenological steps of the process, i.e. the biomass solubilisation and the sugars formation. To this end, for each cellulosic fraction two oligomers were used, one to represent the first soluble oligomer and other

to symbolize the last oligomer before sugar production, which would correspond to the dimer. In addition, the deacetylation of hemicellulose and cellulose were added. The formation of an insoluble oligomer from cellulose was introduced aimed at taking into account those cellulose fractions that could not decompose into sugars at the operating conditions and the char formation from cellulose polymer. Besides, a proton consumption reaction was introduced because at the start of the operation pH increments were observed. So, it is assumed that certain amount of inorganic compounds with basic behaviour was present in biomass. This value was initially fixed at 1% in order to provide enough substance to the neutralization but without disturbing the initial composition a lot. The solubilisation of cellulose and hemicellulose at high temperatures was added too. The formation of degradation products was not taking into account because its value at the operational conditions was very low and they could not be quantified feasibly. Finally, hexoses (C6) formation from cellulose and hemicellulose was also considered.

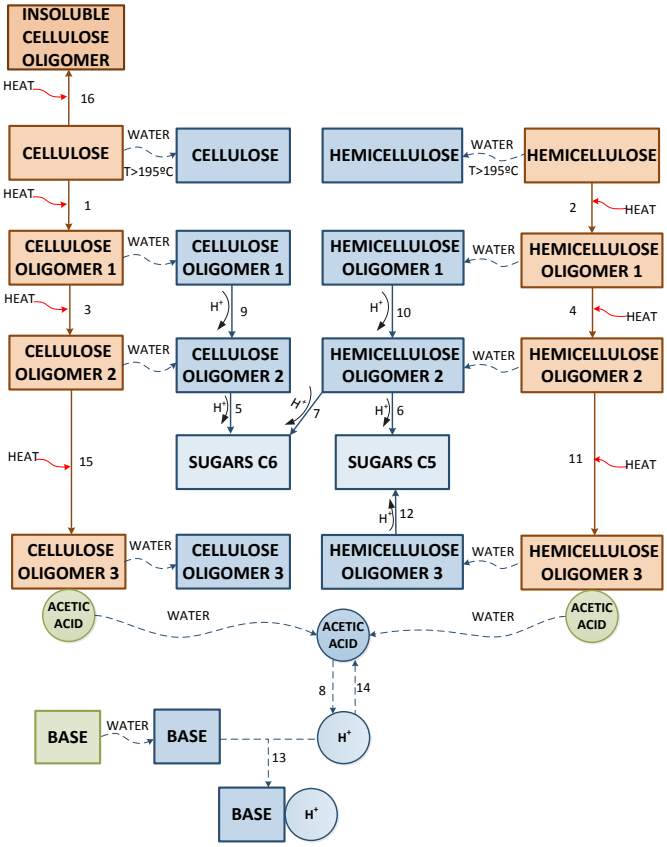

Figure 4: Reaction pathway for the cellulosic fraction of biomass.

3.5. Kinetic model

3.5.1. Assumptions

In order to simplify the modelling the following assumptions were done:

- The solid phase is homogeneous and uniform and it behaves as a whole. Thus, there are neither temperature nor concentration profiles within the solid along the reactor.
- The solid porosity only depends on the total concentration of the solid phase.
- There are not significant diffusional effects in the solid or liquid phase.

- Lignin behaves as an inert, taking as negligible the 2.36% of soluble lignin measured.
- The reaction order for all the kinetics is 1 for the biomass compound. In liquid phase, it is also considered that the kinetics depend on protons concentration with order 1.

3.5.2. Solid phase balances

The model of the fractionation used a non-stationary mass balance for each compound present in biomass assuming that the concentration in the solid could be calculated as the product of the liquid equilibrium concentration and an equilibrium constant ($C_{S_j} = H_j \cdot C_{L_j}^*$), see equation (1):

$$\frac{d(1-\mathcal{E}) \cdot C_{S_j}}{dt} = r_j - k_j \cdot a \cdot (C_{L_j}^* - \bar{C}_{L_j}) \quad (1)$$

Taking into account that the porosity was defined by equation (2), equation (1) could be rewritten in equation (3).

$$\mathcal{E} = 1 - \varphi \cdot C_t \quad (2)$$

$$\frac{dC_{S_j}}{dt} = \frac{1}{1-\mathcal{E}} \cdot \left[r_j - \varphi \cdot C_{S_j} \cdot \frac{dC_t}{dt} - k_j \cdot a \cdot (C_{L_j}^* - \bar{C}_{L_j}) \right] \quad (3)$$

For the inert compound the mass balance is shown in equation (4).

$$\frac{d(1-\mathcal{E}) \cdot \left(C_t - \sum_{j=1}^{j=N} C_{S_j} \right)}{dt} = 0 \quad (4)$$

3.5.3. Liquid phase balances

In the same way that in the solid phase, the model was obtained by the non-stationary mass balance for each compound present in this phase, see equation (5).

$$\frac{\delta \mathcal{E} \cdot C_{L_j}}{\delta t} + \frac{u}{L} \cdot \frac{\delta C_{L_j}}{\delta z} = r_j + k_j \cdot a \cdot (C_{L_j}^* - \bar{C}_{L_j}) \quad (5)$$

And equation (5) could be transformed in equation (6) by introducing the definition of the porosity, given in equation (2).

$$\frac{\delta C_{L_j}}{\delta t} = \frac{1}{\mathcal{E}} \cdot \left[r_j - \frac{u}{L} \cdot \frac{\delta C_{L_j}}{\delta z} - \varphi \cdot C_{L_j} \cdot \frac{dC_t}{dt} + k_j \cdot a \cdot (C_{L_j}^* - \bar{C}_{L_j}) \right] \quad (6)$$

3.5.4. Kinetics

The kinetics for each compound in both phases are given by the generic expression (7).

$$r_j = \sum_{i=1}^{i=n_{reac}} \Phi_{i,j} \cdot r_i \qquad (7)$$

The reaction velocity followed an autocatalytic model, see equation (8). This type of kinetic expression was selected because it has been shown by others authors (Capart et al., 2004) and in a previous work about biomass thermal degradation (Cabeza et al., 2015) that it is able to reproduce big mass changes during a fractionation or depolymerisation process. The parameter $\alpha_{i,j}$ is the initialization factor, and it is used to provide an initial value to the reaction velocity. In this case, it would be a measure of the biomass resistance against fractionation. It was fixed at 0.99 because it is the most recommended (Capart et al., 2004). On the other hand, $\beta_{i,j}$ is the acceleration factor and it represents how fast the mass change is once the decomposition process has started. In this work, it was used to represent the continuous breaking of cellulose and hemicellulose in oligomers of decreasing molecular weight.

$$r_i = k_i \cdot \prod_{j=1}^{j=N} C_{f_j} \cdot \left(1 - \alpha_{i,j} \cdot \frac{C_{f_j}}{C_{f_t}}\right)^{\beta_{i,j}} \qquad (8)$$

Equation (8) was also used to simulate the deacetylation reactions considering that they have a first order dependence with oligomer concentration and an autocatalytic correction with hemicellulose and cellulose (9). The latter was used in order to introduce the effect of the biomass degradation in the releasing of acetic acid.

$$r_i = k_i \cdot \left(1 - \alpha_{i,Cel} \cdot \frac{C_{Cel}}{C_t}\right)^{\beta_{i,Cel}} \cdot \left(1 - \alpha_{i,Hcel} \cdot \frac{C_{Hcel}}{C_t}\right)^{\beta_{i,Hcel}} \cdot C_{S_{LO}} \qquad (9)$$

All the expressions from equation (1) to (9) were used in mass basis. So, the stoichiometric coefficients shown in equation (7) were in mass basis too. For this reason, their absolute value is one except to the acetic acid production and protons formation reactions. In the former, it was assumed that for 1,000 mg g of oligomer 300 mg of acetic acid are produced. For the latter, it was used a relation of 17 mg of released proton per 1,000 mg of acetic acid.

3.6. Discretisation method

It can be observed in the section 3.5 that partial derivate equations (PDE) were used. So, a discretization method along the length of the reactor was needed. The selected method was to divide the length of the reactor in several finite elements and, inside of each of them, to apply the orthogonal collocation method. This method was mainly selected due to the fact that it requires less points (so, less calculating time) than a conventional finite differences method (Press et al., 2007; Villadsen and Stewart, 1995). Generally, the use of finite elements implies a checking of the continuity equation between the limits of each element (Carey and Finlayson, 1975; Press et al., 2007). Nevertheless, it increases the programming necessities and calculating times. Therefore, a modification was used in this work. The idea was to consider the limits of these elements as a normal point of the orthogonal collocation in which the mass balances described in the section 3.5.3 were directly used. This modification was

successfully tested in an adsorption column problem with better results than the finite differences method by comparison with the analytic solution.

Once discretized the system, the obtained set of ordinary differential equation was solved by the Runge-Kutta's method with 8th order of convergence. Because of the high number of adjustable parameters (around 48), a preliminary solution was obtained without any optimization method. It was improved by a Simplex-Nelder-Mead's method using as objective function the addition of the absolute averaged deviations (A.A.D), of the pH, TOC and acetic acid concentration (10).

$$A.A.D. = \sum_{i=1}^{o} \frac{\left|x_{i_{EXP}} - x_{i_{SIM}}\right|}{x_{i_{EXP}}} \cdot 100 \qquad (10)$$

The developed program is available for free in the web page of the research group of high pressure processes of the University of Valladolid (http://hpp.uva.es/software/).

3.7. Process simulation

During the optimization process, all the compounds included in the reaction pathway (Figure 4) were simulated in order to check if the whole obtained behaviour agrees with literature. Therefore, sugar and oligomer concentration evolution as in solid as in liquid phase was calculated.

4. Results and discussion

4.1. Influence of operational conditions in the extraction

The evolution of the extracted mass with the water volumetric flow is depicted in Figure 5. Data were divided into two series depending on the particle diameter. It can be perceived that there is a clear dependence of the process with liquid flow, higher the flow faster and higher extraction was. Which was expected, because the mass transfer is enhanced under those conditions. The potential relation would be also awaited due to the fact that the effect of the flow in mass transfer always tends to a certain limit. Comparing both series it could be concluded that an increment in the particle diameter improved extraction. However, a bigger particle diameter implies, *de facto*, less contact area between solid and liquid. So, mass transfer would be reduced and the extraction should be worse. This discrepancy could be explained by the fact that the data at 3 mm of particle diameter were obtained at temperatures around 180ºC and the data at 6 mm around 190ºC. Therefore, a higher temperature would enhance extraction (due to solubility and kinetic increments) and it would fade the negative effect of using a greater particle diameter. Thus, it is clear that temperature was the most important operational factor. Temperature would be also the cause of the fact that at 9.6 mL/min the extraction had its maximum, because it was at 207ºC. In addition, at these conditions, the real effect of the particle diameter could be checked because temperature and flow were the same in both sets. The result was that a decrement in the diameter improves the extraction, which agrees with the expected behaviour.

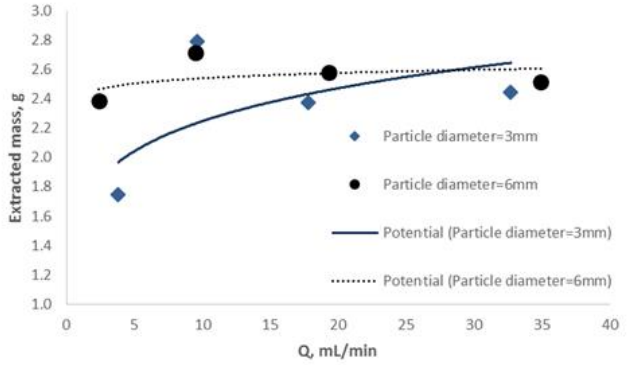

Figure 5: Extracted biomass depending on the liquid flow and particle diameter.

The variation in the maximum measured TOC with the liquid flow is shown in Figure 5. It can be seen that the higher the flow was, the lower TOC was obtained. Thus, high liquid flows mean more dilute output, which could originate problem in a post-treatment of this stream.

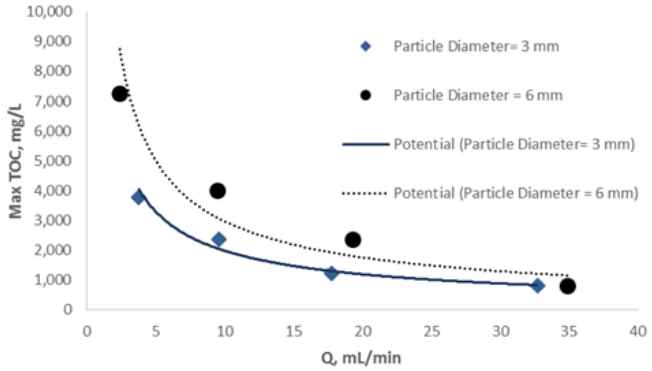

Figure 6: Maximum Toc in liquid phase depending on the liquid flow and particle diameter.

4.2. Fittings

A total of 8 experiments were fitted in order to validate the proposed model. The adjustments of the TOC, acetic acid concentration and pH for the first experiment (Table 2) are shown in Figure 7, Figure 8 and Figure 9 respectively. The simulation of the TOC was multiplied by a conversion factor in order to transform its units (mg of biomass) into mg of carbon. This factor was calculated for each experiment by the division between the integral of the experimental TOC (using the trapezoidal method) and the real extracted mass.

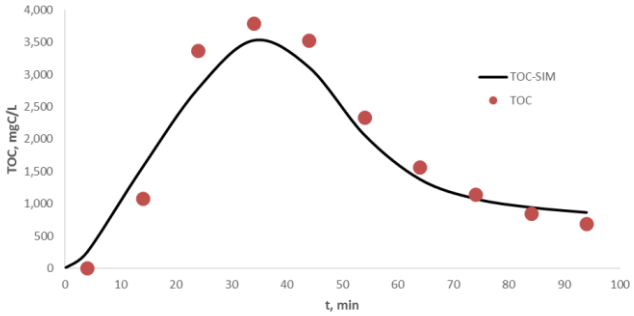

Figure 7: Fitting of the TOC for the first experience. TOC: experimental TOC;. TOC-SIM: simulated TOC.

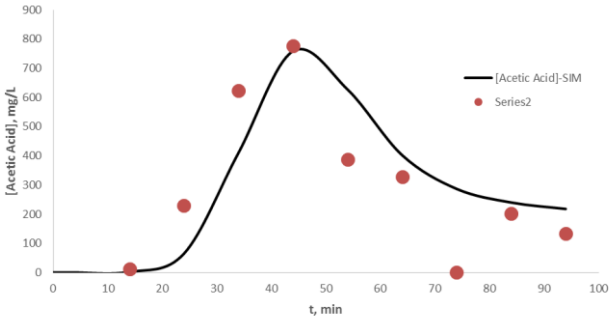

Figure 8: Fitting of the acetic acid concentration in liquid phase for the first experience. [Acetic-Acid]: experimental acetic acid concentration; [Acetic-Acid]-SIM: simulated acetic acid concentration.

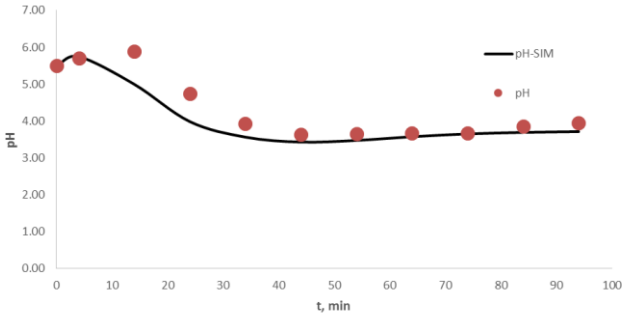

Figure 9: Fitting of the pH for the first experience. pH: experimental pH; pH-SIM: simulated pH.

Figure 7 shows that the extraction had a delay of 4 min. Which was expected because the residence time in this experiment was relatively high (7.8 min) and the temperature was the lowest, 175 ºC. Therefore, biomass needed this 4 min to break until a soluble oligomer. The extraction would continue at the same velocity until 14 min when acetic acid releasing started (Figure 8). This acid production would also explain that at this time the pH reached a maximum (Figure 9). After this emission the extraction rate was enhanced and the TOC grew to their maximum values (time between 24 and 44 min). Therefore, it was confirmed that the production of acetic acid is the main reason of the hydrothermal fractionation. From 44 min, biomass would be highly degraded and the most soluble compound would have been yet removed. For this reason, the TOC and the acetic acid concentration started to decrease. Besides, biomass would be composed each time by compound of lower solubility, which would explain the fact that in the ending of the process the TOC decreased slowly. Finally, it is remarkable that

441 before the acetic acid production pH shows an increment. This behaviour could be
442 caused by some basic compounds present in biomass that would react with protons.
443 As soon as acetic acid is released, this proton consumption is covered up.

444 It can be observed from Figure 7 to Figure 9 that the model was able to reproduce the
445 experimental behaviour of the system in the experiment 1. Including the slight pH
446 increment in the beginning of the operation. The absolute averaged deviations (A.A.D.)
447 between the experimental data end the simulation were calculated by equation (10).
448 The result for each of them was TOC (16.3%), pH (6.6%) and acetic acid (44.4%),
449 values that could be acceptable due to the experimental variability of biomass. The
450 reason of the higher discrepancy in the acetic acid concentration could be caused by
451 the fact the experimental methods used to determinate it has a relatively low precision.
452 However, the pH, which depends on this concentration directly, has an error lower than
453 7%. So, the acetic acid prediction was assumed as correct.

454 The rest of experiments were also fitted and their A.A.D. are arrayed in Table 3.

455 *Table 3: Fittings A.A.D.*

Experiment	A.A.D. TOC %	A.A.D. pH %	A.A.D. Acetic acid concentration %
1	16.3	6.6	44.4
2	20.8	9.3	84.4
3	23.4	5.7	45.7
4	55.8	8.8	49.5
5	24.9	6.4	*
6	16.7	6.8	*
7	44.2	5.6	*
8	54.8	9.7	*

456 **No experimental data available.*

457 From the data collected in Table 2 and Table 3 it can be concluded that the higher the
458 flow was, the higher errors in TOC and acetic acid concentration were. Which could be
459 originated by a loss of precision in the experimental method due to the higher dilution
460 of the samples (Figure 5). Other possible reason would be the strong changes in the
461 extraction rate due to temperature. However, the discrepancies are low taking into
462 account the complexity of the problem.

463 *4.2.1. Kinetic parameters*

464 In order to test if the kinetic constants would follow the Arrhenius' law, a lineal
465 regression of each of them was done (Figure 10 and Figure 11).

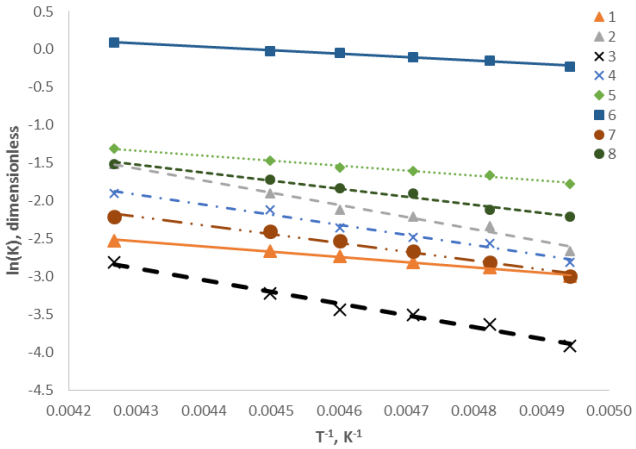

Figure 10: Linear regression for the kinetics from reaction 1 to 8.

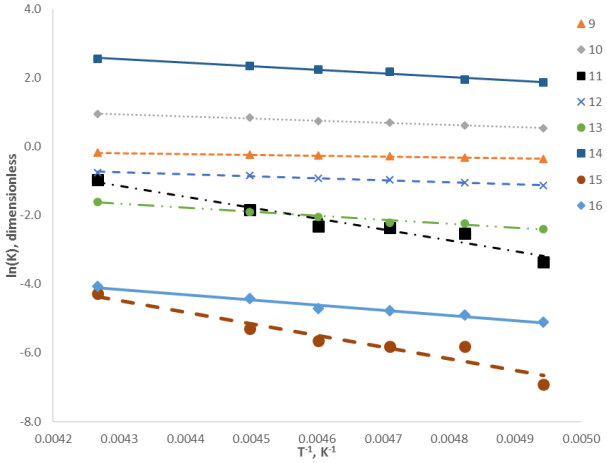

Figure 11: Linear regression for the kinetics from reaction 9 to 16.

Table 4 shows the calculated Arrhenius' pre-exponential factor and the activation energy. In addition, the R^2 of all of them was also obtained and in all the cases it was greater than 0.9129. So, it was confirmed that kinetics followed the Arrhenius' law.

Table 4: Kinetic constant parameters.

Reaction	ln(k)	Ea/R K	R^2
1	0.4284	689	0.9935
2	5.3180	1603	0.9815
3	3.7349	1542	0.9804
4	3.8512	1340	0.9816
5	1.5075	662	0.9905
6	2.0488	458	0.9951
7	2.8218	1169	0.9861
8	3.0058	1053	0.9803
9	0.8864	250	0.9939
10	3.6587	632	0.9961
11	12.5630	3187	0.9445

12	1.7045	571	0.9821
13	3.3634	1170	0.9843
14	7.0680	1053	0.9803
15	10.1160	3392	0.9129
16	2.3708	1516	0.9800

Table 5 and Figure 12 show the values for the acceleration factors which were different form cero. $\beta_{1,Co1}$ and $\beta_{2,Co2}$ increased their values with temperature and flow. Which was expected because they were used to simulate the biomass breaking into oligomers of decreasing molecular weight. And, if temperature or flow are increased, this breaking would be more abrupt. So, higher acceleration factor would be needed. On the other hand, $\beta_{11,Co1}$, $\beta_{11,Co2}$, $\beta_{15,Co1}$ and $\beta_{15,Co2}$ showed the opposite behaviour. This could be caused by the fact that they were used to simulate the effect of the biomass degradation in acetic acid production. So, with higher temperatures and flows, the releasing would be faster. It is remarkable that $\beta_{11,Co1}$, $\beta_{11,Co2}$, $\beta_{15,Co1}$ and $\beta_{15,Co2}$ have the same values. This was caused by the fact that all of them represent the acetic acid formation.

Table 5: Acceleration factors.

Experiment	$\beta_{1,Co1}$	$\beta_{2,Co2}$	$\beta_{11,Co1}$	$\beta_{11,Co2}$	$\beta_{15,Co1}$	$\beta_{15,Co2}$
1	2.2	9.0	11.0	11.0	11.0	11.0
2	3.0	10.5	7.0	7.0	7.0	7.0
3	4.0	12.0	4.5	4.5	4.5	4.5
4	3.5	11.0	4.0	4.0	4.0	4.0
5	2.5	10.0	10.0	10.0	10.0	10.0
6	3.0	10.5	7.0	7.0	7.0	7.0
7	4.1	12.5	4.0	4.0	4.0	4.0
8	3.5	11.0	3.8	3.8	3.8	3.8

Co1: cellulose; Co2: hemicellulose.

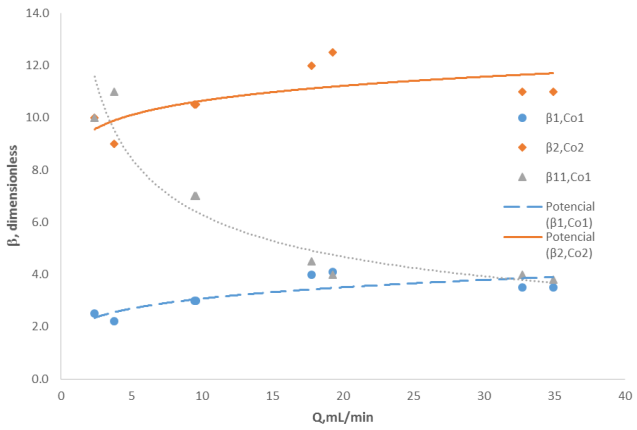

Figure 12: Acceleration factors evolution. $\beta_{11,Co1}$ was only represented because it had the same values that $\beta_{11,Co2}$, $\beta_{15,Co1}$ and $\beta_{15,Co2}$.

4.2.2. Mass transfer parameters

Table 6 collects the calculated values of the equilibrium constants for the soluble components at the studied temperatures. The relation with temperature was confirmed as linear by a regression analysis whose coefficient R^2 was ever greater than 0.9507 (Figure 13). It is remarkable that compound 1 and 2 (cellulose and hemicellulose respectively) would start to solve at temperatures greater than 195ºC. This could be explained by changes in the polarity of the water with temperature.

Table 6: Equilibrium constants (dimensionless) between solid and liquid phases.

T ºC	Co1	Co2	Co3	Co4	Co5	Co6	Co10	Co12 [1]	Co13
190	0.00	0.00	0.34	0.40	0.34	0.52	3.50	0.15	0.08
175	0.00	0.00	0.10	0.15	0.10	0.30	2.00	0.03	0.05
195	0.15	0.10	0.40	0.48	0.40	0.58	4.00	0.20	0.09
185	0.00	0.00	0.24	0.27	0.24	0.36	3.00	0.09	0.07
180	0.00	0.00	0.13	0.16	0.13	0.30	2.50	0.06	0.06
207	0.50	0.45	0.52	0.63	0.52	0.72	4.80	0.28	0.12
R^2	-	-	0.9724	0.9715	0.9724	0.9507	0.9902	0.9886	0.9963

Co1: cellulose; Co2: hemicellulose; Co3: cellulose oligomer 1 (first oligomer soluble from cellulose); Co4: hemicellulose oligomer 1 (first oligomer soluble from hemicellulose); Co5: cellulose oligomer 2 (last oligomer from cellulose before sugar production); Co6: hemicellulose oligomer 2 (last oligomer from hemicellulose before sugar production); Co10: acetic acid; Co12: hemicellulose oligomer 3 (deacetylated oligomer from hemicellulose); Co15: cellulose oligomer 3 (deacetylated oligomer from cellulose); Co13: base (inorganic compound). [1]*Compound 12 and 15 had the same equilibrium constant.*

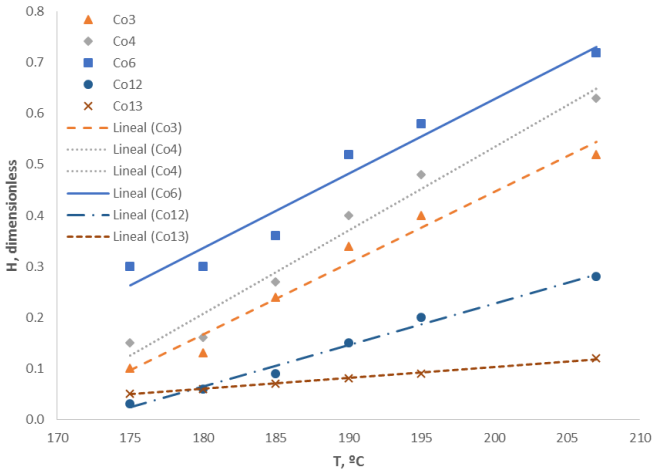

Figure 13: Equilibrium constant evolution with temperature. Compound 5 and 15 were not showed because they had the same equilibrium constant that compound 3 and 12 respectively.

Table 7 and Table 8 shows the calculated mass transfer coefficients (multiplied by the specific exchange area) obtained from the adjustments. Table 7 have the parameters with a particle diameter of 3 mm and Table 8 with a particle diameter of 6 mm. The necessity of use two sets of parameters would be explained by the fact that the

exchange area depends on the particle diameter. In addition, it was checked the relation between them and the liquid flow. And it resulted as linear with R^2 higher than 0.9434. The changes of these mas transfer coefficients are represented in Figure 14 and Figure 15 for 3 mm and 6 mm respectively.

Table 7: Mass transfer coefficients ($min^{-1} \cdot 10^2$) with a particle diameter of 3mm.

Q mL/min	Co1	Co2	Co3	Co4	Co5	Co6	Co10	Co12[1]	Co13
3.8	0.0	0.0	2.6	15	2.6	22	200	1.5	0.9
9.6	1.1	1.1	3.0	18	3.0	25	220	1.6	1.2
17.8	0.0	0.0	4.0	20	4.0	27	340	1.8	1.5
32.7	0.0	0.0	8.0	26	8.0	37	500	2.1	2.0
R^2	-	-	0.9434	0.9905	0.9434	0.9795	0.9825	0.9980	0.9923

Co1: cellulose; Co2: hemicellulose; Co3: cellulose oligomer 1 (first oligomer soluble from cellulose); Co4: hemicellulose oligomer 1 (first oligomer soluble from hemicellulose); Co5: cellulose oligomer 2 (last oligomer from cellulose before sugar production); Co6: hemicellulose oligomer 2 (last oligomer from hemicellulose before sugar production); Co10: acetic acid; Co12: hemicellulose oligomer 3 (deacetylated oligomer from hemicellulose); Co15: cellulose oligomer 3 (deacetylated oligomer from cellulose); Co13: base (inorganic compound). [1]Compound 12 and 15 had the same mass transfer coefficient.

Table 8: Mass transfer coefficients ($min^{-1} \cdot 10^2$) with a particle diameter of 6 mm.

Q mL/min	Co1	Co2	Co3	Co4	Co5	Co6	Co10	Co12[1]	Co13
2.4	0.0	0.0	2.4	14	2.4	20	180	1.4	0.8
9.5	1.0	1.0	2.5	15	2.5	24	215	1.5	1.1
19.3	1.5	1.5	4.5	16	4.5	30	350	2.0	1.5
34.9	0.0	0.0	8.2	18	8.2	38	520	2.3	2.0
R^2	-	-	0.9522	0.9978	0.9522	0.9984	0.9868	0.9583	0.9956

Co1: cellulose; Co2: hemicellulose; Co3: cellulose oligomer 1 (first oligomer soluble from cellulose); Co4: hemicellulose oligomer 1 (first oligomer soluble from hemicellulose); Co5: cellulose oligomer 2 (last oligomer from cellulose before sugar production); Co6: hemicellulose oligomer 2 (last oligomer from hemicellulose before sugar production); Co10: acetic acid; Co12: hemicellulose oligomer 3 (deacetylated oligomer from hemicellulose); Co15: cellulose oligomer 3 (deacetylated oligomer from cellulose); Co13: base (inorganic compound). [1]Compound 12 and 15 had the same mass transfer coefficient.

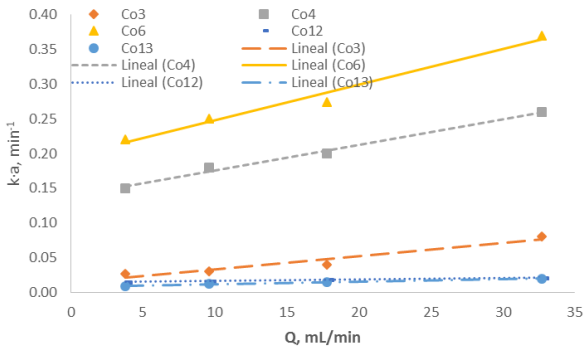

Figure 14: Mass transfer coefficients evolution with liquid flow for a particle diameter of 3 mm. Compound 5 and 15

were not showed because they had the same mass transfer coefficient that compound 3 and 12 respectively.

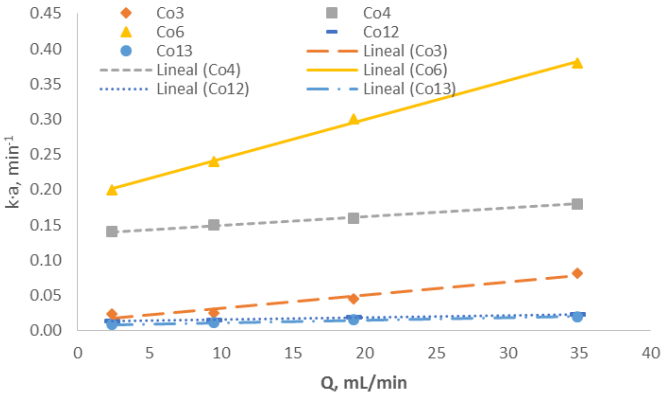

Figure 15: Mass transfer coefficients evolution with liquid flow for a particle diameter of 6 mm. Compound 5 and 15 were not showed because they had the same mass transfer coefficient that compound 3 and 12 respectively.

4.3. Simulated behaviour

As it was mentioned in part 3.7, a simulation of the solid and liquid phase was performed in order to compare it with the experimental behaviour showed by others authors. In Figure 16 it is shown the breaking of cellulose in solid phase for the first experiment. It can be observed that the cellulose would decompose first into the first soluble oligomer which would break into the last oligomer before the sugar formation. In addition, this last oligomer would break into acetic acid and a deacetylated oligomer. In parallel, the formation of insoluble oligomer would take place too. At the end of the operation, cellulose would be present only as oligomers and the variation of the cellulose mas would be of 29%. Hemicellulose breaking was simulated too. The behaviour was similar to the cellulose but the variation of the concentration was higher (86%). The 14% of hemicellulose that remained in solid would be as deacetylated oligomer due to their lower solubility.

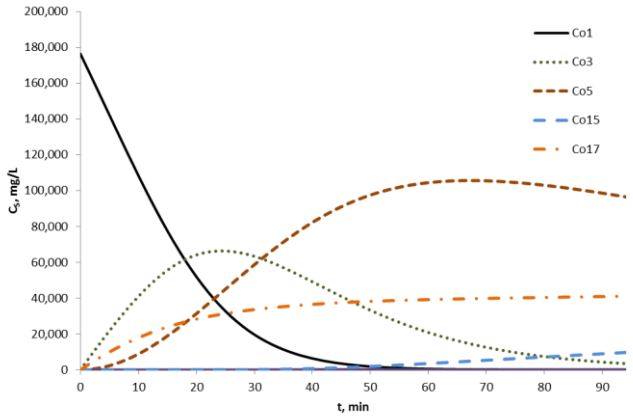

Figure 16: Cellulose breaking in solid phase. Co1: cellulose; Co3: cellulose oligomer 1 (first oligomer soluble from cellulose); Co5: cellulose oligomer 2 (last oligomer from cellulose before sugar production); Co15: cellulose oligomer 3 (deacetylated oligomer from cellulose); Co17: insoluble cellulose oligomer.

Figure 17 shows the simulation of the hemicellulose oligomers decomposition in liquid phase for the experiment 1. It is remarkable that the main part of biomass is extracted as oligomer and that at the end of the process, only sugars would be obtained.

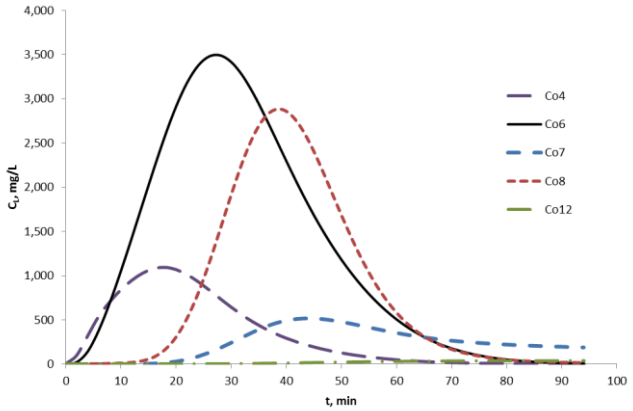

Figure 17: Hemicellulose oligomers breaking in liquid phase. Co4: hemicellulose oligomer 1 (first oligomer soluble from hemicellulose); Co6: hemicellulose oligomer 2 (last oligomer from hemicellulose before sugar production); Co7: Sugars C6; Co8: Sugars C5; Co12: hemicellulose oligomer 3 (deacetylated oligomer from hemicellulose).

The simulations of the rest of the experiments were performed too. The maximum conversion of hemicellulose and cellulose was achieved in the experiment 2, 94% and 61% respectively. These results would be expected because it was done at the highest temperature (207ºC) and with the lowest particle diameter (3mm). In addition, it confirms the idea of temperature is the main process variable, which was also exposed in the section 4.1.

Hemicellulose results agree with the behaviour reported by other authors. *M. Sefik Tunc et al.* (M. Sefik Tunc, 2008) studied the hydrothermal fractionation of hardwood biomass at 150ºC for 500 min. They found that cellulose was not extracted at any time and that around 67 % hemicellulose was recovered at 500 min (23% at 100 min). In addition, they reported that the main of the extracted biomass was as oligomer and that at the end of the process only monomers were obtained. *Carl Pronyk et al.* (Pronyk and Mazza, 2010) assessed the hydrothermal fractionation of triticale straw also at 150ºC and they obtained similar results to *M. Sefik Tunc et al.* *Jussi V. Rissanen et al.*(Rissanen et al., 2014) analysed the hemicellulose extraction from spruce from 120ºC to 170ºC, recovering 80% of hemicellulose at 170ºC with an operating time of 50 min. Regarding cellulose, the calculated yields were higher than the reported by other authors. *Mohd Rafein Zakaria et al.(Zakaria et al., 2015)* obtained yield around 15% at 180ºC and 23% at 210ºC (both after 10 min of operation in batch reactor). *Patrícia Moniz* et al.(Moniz et al., 2013) performed experiments also in a batch reactor and the extraction of cellulose at 170ºC was 6.2% and at 200ºC 9.8%. These discrepancies could be explained by the fact that our system was a semi-continuous process, which could enhance mass transfer and cellulose breaking, with operating time longer than 10 min (94 min). Besides, the pH suffered variations during the process in our reactor which could enhance the cellulose fractionation. The pH decreased down to 3.65 in the experiment 1 and until 3.78 in the experiment 2. In addition, it was less than 4 from 34 min to 94 min for the former and lower than 4.5 from 24 min to 94 min for the latter.

Moreover, the total amount of hemicellulose in the sample was around 1g and the measured extracted mass was between 1.6 g and 2.8 g (Figure 5). So, a considerable amount of cellulose should be extracted.

Finally, the mass balance between the solid and liquid phase was checked. Table 9 arrays the values of the final mass in the solid after the extraction calculated by simulation and the experimental data. The discrepancies are lower than 8.5%. Besides, the average difference between the simulated and experimental final mass was 0.1189 g and the average soluble lignin was 0.1253 g. Therefore, the main part of these differences (and of the TOC deviations) would be caused by this soluble lignin considered as inert.

Table 9: Comparison between the simulated and experimental final mass in the solid.

Experiment	m_{real} g	m_{sim} g	Discrepancy %
1	3.5656	3.6333	1.90
2	2.5278	2.7324	8.09
3	2.9585	3.0238	2.21
4	2.8148	2.8345	0.70
5	2.8736	3.1070	8.12
6	2.6857	2.8498	6.11
7	2.6739	2.7401	2.48
8	2.7061	2.8366	4.82

5. Conclusions

A kinetic model for the two-phase simulation of the hydrothermal fractionation of holm oak has been developed. The kinetic constants follow the Arrhenius' law and the mas transfer coefficients and equilibrium constant have a linear dependency with flow and temperature respectively. This model can reproduce the TOC, pH and acetic acid concentration with relative low differences. The deviations are between 16.3% and 55.8% for the TOC, between 5.6% and 9.7% for the pH and between 44.4% and 84.4% for the acetic acid. Besides it is able to simulate the behaviour in solid and liquid phase in agreement with the experimental data reported by other authors. The mass balance between the solid and the liquid was calculated with deviations lower than 8.5%, which are mainly caused by the fact that soluble lignin is not considered. It is remarkable that cellulose extraction is much higher than expected. However, this result can be explained by the fact that the system is a semi-continuous process with high operating times and a strong drop of the pH. Moreover, the main parameters that could affect mass transfer, e. g. particle diameter, volumetric flow and temperature, are studied. Being temperature the most important of them. It would be interesting in a future work to introduce the degradation product formation in the model and the released sugars. Unfortunately, that would require to increase the number of fittings parameter even more. Therefore, another approach should be considered to perform a more detailed study. The best option would be a poblational model in which activation energies and solubility of the oligomers were function of their molecular weight.

Acknowledgements

The authors acknowledge the Spanish Economy and Competitiveness Ministry, Project Reference: ENE2012-33613 and the regional government (Junta de Castilla y León), Project Reference: VA330U13 for funding. Álvaro Cabeza would like to thank to the Spanish Ministry of Education Culture and Sports, training program of university professors (reference FPU2013/01516) for the research training contract.

Nomenclature

Acronyms

Co1: Cellulose.

Co2: Hemicellulose.

Co3: Cellulose oligomer 1 (first oligomer soluble from cellulose).

Co4: Hemicellulose oligomer 1 (first oligomer soluble from hemicellulose).

Co5: Cellulose oligomer 2 (last oligomer from cellulose before sugar production).

Co6: Hemicellulose oligomer 2 (last oligomer from hemicellulose before sugar production).

Co7: Sugars C6.

Co8: Sugars C5.

Co10: Acetic acid.

Co12: Hemicellulose oligomer 3 (deacetylated oligomer from hemicellulose).

Co13: Base (inorganic compound).

Co15: Cellulose oligomer 3 (deacetylated oligomer from cellulose).

Co17: Insoluble cellulose oligomer.

TOC: Total Organic Content.

A.A.D.: Average absolute Deviation.

Subindex and superindex

pH-SIM: Simulated pH.

pH: Experimental pH.

TOC-SIM: Simulated TOC.

TOC: Experimental TOC.

[Acetic acid]-SIM: Simulated acetic acid concentration.

[Acetic acid]: Experimental acetic acid concentration.

Greek letters and symbols

$\mathcal{E}$: Porosity of the bed, dimensioless.

C_{S_j}: Cocnetration of the compound "j" in the solid phase, mg/L.

r_j: Reaction rate of the compound "j", mg/min·L.

$k_j \cdot a$: Mass transfer coefficient multiplied by the specific exchange area, min^{-1}.

$C_{L_j}^*$: Equilibrium concentration of the compound "j" in liquid phase, mg/L.

$\bar{C}_{L_j}$: Average concentration of the compound "j" along the reactor in liquid phase, mg/L.

H_j: Equilibrium constant between the solid and the liquid, dimensionless.

C_t: Total concentration in the solid, mg/L.

φ: Relation factor between porosity and the total concentration in solid phase, dimensionless.

C_{L_j}: Concentration of the compound "j" in the liquid phase, mg/L.

$\Phi_{i,j}$: Stoichiometric coefficient of the compound "j" for the reaction "i", mg.

r_i: Reaction velocity "i", mg/min·L.

$\alpha_{i,j}$: Initial velocity factor for the compound "j" in the reaction "i", dimensionless.

$\alpha_{i,Cel}$: Initial velocity factor for cellulose in the reaction "i", dimensionless.

$\alpha_{i,Hcel}$: Initial velocity factor for hemicellulose in the reaction "i", dimensionless.

$\beta_{i,j}$: Acceleration factor for the compound "j" in the reaction "i", dimensionless.

$\beta_{i,Cel}$: Acceleration factor for cellulose in the reaction "i", dimensionless.

$\beta_{i,Hcel}$: Acceleration factor for hemicellulose in the reaction "i", dimensionless.

k_i: Kinetic constant, $mg^{-1} \cdot min^{-1}$.

C_{f_j}: Concentration of the compound "j" in the phase "f", mg/L.

C_{Cel}: Concentration of cellulose in the solid phase, mg/L.

C_{Hcel}: Concentration of hemicellulose in the solid phase, mg/L.

$C_{S_{LO}}$: Concentration of the last oligomer before sugar production (from hemicellulose or cellulose) in the solid phase, mg/L.

u: Liquid velocity in the reactor, m/min.

N: Number of compounds, dimensionless.

n_{rec}: Number of reactions, dimensionless.

L: Length of the reactor, m.

z: Coordinate along the length of the reactor, dimensionless.

t: Operating time, min.

713 $x_{i_{EXP}}$: Experimental value of the fitted variable.

714 $x_{i_{SIM}}$: Simulated value of the fitted variable.

715 o: Total number of experiments, dimensionless.

716 k: Pre-exponential factor of the kinetic constant, $mg^{-1} \cdot min^{-1}$.

717 Ea/R: Activation energy, K.

718 R^2: Coefficient R^2, dimensionless.

719 T: Operating temperature, ºC.

720 m_{real}: Final solid mass, g.

721 m_{sim}: Simulated final solid mass, g.

722

723 **List of figures**

cellulose before sugar production); Co15: cellulose oligomer 3 (deacetylated oligomer from cellulose); Co17: insoluble cellulose oligomer.
Figure 17: Hemicellulose oligomers breaking in liquid phase. Co4: hemicellulose oligomer 1 (first oligomer soluble from hemicellulose); Co6: hemicellulose oligomer 2 (last oligomer from hemicellulose before sugar production); Co7: Sugars C6; Co8: Sugars C5; Co12: hemicellulose oligomer 3 (deacetylated oligomer from hemicellulose).

List of tables

References

Alvarez-Vasco, C., Zhang, X., 2013. Alkaline hydrogen peroxide pretreatment of softwood: Hemicellulose degradation pathways. Bioresource Technology 150, 321-327.

Asl, A.H., Khajenoori, M., 2013. Subcritical Water Extraction, Mass Transfer - Advances in Sustainable Energy and Environment Oriented Numerical Modeling. InTech.

Bobleter, O., 1994. Hydrothermal degradation of polymers derived from plants. Progress in Polymer Science (Oxford) 19, 797-841.

Cabeza, A., Sobrón, F., Yedro, F.M., García-Serna, J., 2015. Autocatalytic kinetic model for thermogravimetric analysis and composition estimation of biomass and polymeric fractions. Fuel 148, 212-225.

Cantero, D.A., Bermejo, M.D., Cocero, M.J., 2013. Kinetic analysis of cellulose depolymerization reactions in near critical water. The Journal of Supercritical Fluids 75, 48-57.

Capart, R., Khezami, L., Burnham, A.K., 2004. Assessment of various kinetic models for the pyrolysis of a microgranular cellulose. Thermochimica Acta 417, 79-89.

Carey, G.F., Finlayson, B.A., 1975. Orthogonal collocation on finite elements. Chemical Engineering Science 30, 587-596.

Charles, E.W., Stephen, R.D., Michael, E.H., John, W.B., Catherine, E.S., Liisa, V., 2004. Hydrolysis of Cellulose and Hemicellulose, Polysaccharides. CRC Press.

Feng, Y., Qi, X., Jian, H.L., Sun, R.C., Jiang, J.X., 2012. Effect of inhibitors on enzymatic hydrolysis and simultaneous saccharification fermentation for lactic acid production from steam explosion pretreated lespedeza stalks. BioResources 7, 3755-3766.

Franck, E.U., 1970. Water and aqueous solutions at high pressures and temperatures. Pure Appl. Chem 24, 13-30.

801 Gao, P., Li, G., Yang, F., Lv, X.N., Fan, H., Meng, L., Yu, X.Q., 2013. Preparation of
802 lactic acid, formic acid and acetic acid from cotton cellulose by the alkaline pre-
803 treatment and hydrothermal degradation. Industrial Crops and Products 48, 61-67.

804 Garrote, G., Domínguez, H., Parajó, J.C., 2002. Interpretation of deacetylation and
805 hemicellulose hydrolysis during hydrothermal treatments on the basis of the severity
806 factor. Process Biochemistry 37, 1067-1073.

807 King, D., 2009. The future of industrial biorefineries. Worl Economic Forum.

808 Kruse, A., Dinjus, E., 2007. Hot compressed water as reaction medium and reactant:
809 Properties and synthesis reactions. The Journal of Supercritical Fluids 39, 362-380.

810 M. Sefik Tunc, A.R.P.v.H., 2008. Hemicellulose extraction of mixed southern hardwood
811 with water at 150 °C: Effect of time. Industrial & Engineering Chemistry Research 47,
812 7031-7037.

813 Miller-Chou, B.A., Koenig, J.L., 2003. A review of polymer dissolution. Progress in
814 Polymer Science 28, 1223-1270.

815 Moniz, P., Pereira, H., Quilhó, T., Carvalheiro, F., 2013. Characterisation and
816 hydrothermal processing of corn straw towards the selective fractionation of
817 hemicelluloses. Industrial Crops and Products 50, 145-153.

818 OCDE, 2009. The Bioeconomy to 2030: designing a policy agenda.

819 Organisation, T.E.P.S., 2011. THE EUROPEAN BIOECONOMY IN 2030. Delivering
820 Sustainable Growth by addressing the Grand Societal Challenges, pp. 1-24.

821 P. Harmsen, W.H., L. Bermudez, R. bakker, 2010. Literature review of physical and
822 chemical pretreatment processes for lignocellulosic biomass. Wageningen UR Food &
823 Biobased Research.

824 Parajó, J.C., Garrote, G., Cruz, J.M., Dominguez, H., 2004. Production of
825 xylooligosaccharides by autohydrolysis of lignocellulosic materials. Trends in Food
826 Science & Technology 15, 115-120.

827 Press, W., Teukolsky, S., Vetterling, W., Flannery, B., 2007. Numerical recipes 3rd
828 edition: The art of scientific computing.

829 Pronyk, C., Mazza, G., 2010. Kinetic modeling of hemicellulose hydrolysis from triticale
830 straw in a pressurized low polarity water flow-through reactor. Industrial and
831 Engineering Chemistry Research 49, 6367-6375.

832 Rissanen, J.V., Grénman, H., Willför, S., Murzin, D.Y., Salmi, T., 2014. Spruce
833 hemicellulose for chemicals using aqueous extraction: Kinetics, mass transfer, and
834 modeling. Industrial and Engineering Chemistry Research 53, 6341-6350.

835 Rivas, S., González-Muñoz, M.J., Santos, V., Parajó, J.C., 2014. Acidic processing of
836 hemicellulosic saccharides from pine wood: Product distribution and kinetic modeling.
837 Bioresource Technology 162, 192-199.

838 Sasaki, M., Furukawa, M., Minami, K., Adschiri, T., Arai, K., 2002. Kinetics and
839 mechanism of cellobiose hydrolysis and retro-aldol condensation in subcritical and
840 supercritical water. Industrial and Engineering Chemistry Research 41, 6642-6649.

841 Teo, C.C., Tan, S.N., Yong, J.W.H., Hew, C.S., Ong, E.S., 2010. Pressurized hot water
842 extraction (PHWE). Journal of Chromatography A 1217, 2484-2494.

843 Villadsen, J.V., Stewart, W.E., 1995. Solution of boundary-value problems by
844 orthogonal collocation. Chemical Engineering Science 50, 3981-3996.

845 Yoon, S.Y., Han, S.H., Shin, S.J., 2014. The effect of hemicelluloses and lignin on acid
846 hydrolysis of cellulose. Energy 77, 19-24.

847 Zakaria, M.R., Hirata, S., Hassan, M.A., 2015. Hydrothermal pretreatment enhanced
848 enzymatic hydrolysis and glucose production from oil palm biomass. Bioresource
849 Technology 176, 142-148.

850